THE ASTROPHYSICAL JOURNAL SUPPLEMENT SERIES, 91:613–624, 1994 April

[C II] 158 MICRON AND [O I] 63 MICRON OBSERVATIONS OF THE GALACTIC CENTER REGION

KOHEI MIZUTANI,[1] TOSHINORI MAIHARA,[2] HIDEO MATSUHARA,[3] TAKAO NAKAGAWA,[4] HIROSHI SHIBAI,[4] HARUYUKI OKUDA,[4] YUKIYASU KOBAYASHI,[5] NORIHISA HIROMOTO,[1] TETSUO NISHIMURA,[5] AND FRANK J. LOW[6]

Received 1991 April 3; accepted 1993 August 13

ABSTRACT

Using the balloon-borne infrared telescope (BIRT) incorporated with a liquid-helium–cooled double-channel Fabry-Perot spectrometer, intensities and velocity profiles of [C II] 158 μm and [O I] 63 μm fine-structure lines have been observed in the Galactic center region within $|l| \leqq 0°.7$. Intense [C II] line emission has been detected ubiquitously in almost all of the observed points. The distribution of the [C II] intensity shows a central peak at Sgr A West together with two prominent peaks at $\Delta 1 = \pm 0°.6$, which correspond to Sgr B1 (not Sgr B2) and Sgr C, respectively. The intensity distribution resembles but is not identical to, that of far-infrared emission.

The velocity profiles of the [C II] line are resolved and can be deconvolved into multiple components, many of which can be traced to the features observed by molecular lines. The [O I] 63 μm line has been detected at Sgr A West and at some other points. The [O I] 63 μm/[C II] 158 μm ratios are always less than 3 in the beam of 3'.7.

These observed results can be explained as the emission generated in photodissociation regions formed in the molecular clouds complexes illuminated by intense UV radiation field in the Galactic center regions. However, contribution from ELD region is possibly present and cannot be ruled out.

Subject headings: Galaxy: center — infrared: ISM: lines and bands — ISM: kinematics and dynamics

1. INTRODUCTION

The central region of the Galaxy has long been one of the most intriguing objects. About 10% of the total far-infrared luminosity of the Galaxy is radiated within 250 pc from the center. The molecular gas in this region amounts to 10% of the neutral gas mass of the Galaxy (e.g., Cox & Mezger 1988; Güsten 1989; Cox & Laureijs 1989). The molecular clouds, strong radio sources, and far-infrared emission are concentrated in a narrow ridge ($\Delta b \sim 0°.3$) along the Galactic plane (e.g., Odenwald & Fazio 1984; Handa et al. 1987; Heiligman 1987). The molecular gases in the Galactic center have peculiar characteristics, i.e., temperature of the gas is higher (>60 K) than that of the dust, and the line widths are broader (>10–20 kms^{-1}) than those expected from thermal broadening (e.g., Güsten 1989). Many intriguing features such as Sgr A (West and East), the Radio Arc, the arched filaments, and the ring structures of gases and dust have been found exclusively in the central region. A number of models of the central structures have been proposed but are not yet well understood (e.g., Brown & Listz 1984; Güsten 1989; Sofue 1989).

In this paper, we present some new features observed by the fine-structure line of C^+ at 157.7 μm and of that of 0^0 at 63.2 μm in the central region within $|l| \leqq 0°.7$. These two fine-structure lines are major coolants of UV-illuminated molecular clouds, the so-called "photodissociation regions (PDRs)" (de Jong, Dalgarno, & Boland 1980; Tielens & Hollenbach 1985).

PDRs have been observed in a number of H II regions/molecular clouds complexes (e.g., Genzel, Harris, & Stutzki 1989) and have also been observed in the Galactic central region within 10 pc (Genzel et al. 1984, 1985, hereafter GWCT; Lugten et al. 1986, hereafter LGCT; Poglitsch et al. 1991). These observations are, however, limited in a small area close to the center.

Recently, the PDRs have been found to be one of the major phases of interstellar gas from the observations of the [C II] line in the Galactic disk (Stacey et al. 1985; Shibai et al. 1991) as well as in external galaxies (Crawford et al. 1985; Stacey et al. 1991).

Preliminary results of the observations have been reported previously (Okuda et al. 1989), but here we will present more detailed morphological comparisons with relevant observations in other wavelengths together with discussion on emission mechanisms based on more detailed analyses of the data. Hereafter, we assume the distance to the Galactic center is 8.5 kpc, so that 1' corresponds to 2.5 pc in linear scale.

2. OBSERVATIONS

The observations were made by the 50 cm Balloon-borne Infrared Telescope, BIRT, (Okuda et al. 1984; Shibai et al. 1990). The telescope is mounted on an altazimuth pointing system and a spectrometer is set at its Nasmyth focus. By using an offset guiding system, an absolute pointing accuracy better than 1' ($p - p$) and pointing stability of 30" ($p - p$) were achieved referring to a nearby bright star.

The balloon flights were made on May 25 UT and June 5 UT in 1988 from the National Scientific Balloon Facility

[1] Communications Research Laboratory, 4-2-1, Nukui-kitamachi, Koganei, Tokyo 184, Japan.
[2] Department of Physics, Kyoto University, Kitashirakawa, Sakyo-ku, Kyoto 606, Japan.
[3] Department of Physics, Nagoya University, Furo-cho, Chikusa-ku, Nagoya 464, Japan.
[4] Institute of Space and Astronautical Science, 3-1-1, Yoshinodai, Sagamihara, Kanagawa 229, Japan.
[5] National Astronomical Observatory of Japan, 2-21-1, Osawa, Mitaka, Tokyo 181, Japan.
[6] Steward Observatory, University of Arizona, Tucson, AZ 85721.

(NSBF) at Palestine, Texas. Due to a contingent balloon control, the observing altitude level in the first flight was changed from 26 to 21 km, but in the second flight it was always kept at 31 km. The total observation times used for the Galactic center were 1.5 hr in the first flight and 1 hr in the second flight.

The spectrometer used in the observations is a double-channel Fabry-Perot interferometers, one channel for [C II] 158 μm line and the other for [O I] 63 μm line (Okuda et al. 1986; Nakagawa et al. 1990). Each is a two-stage tandem Fabry-Perot interferometers, composed of a fixed etalon used for sorting of the objective line and a scanable etalon to sweep the wavelength. A common beam from the telescope is introduced to the two interferometers by a beam splitter, and hence the two spectra were observed simultaneously. All optical elements of the spectrometers, the mirrors, the etalons as well as the detectors were cooled by liquid helium to a temperature of 1.8 K.

The velocity resolutions of the spectrometer were 143 kms^{-1} for the [C II] 158 μm line channel and 176 kms^{-1} for the [O I] 63 μm line channel, respectively. The sweeping spectral ranges were from -560 to $+620$ kms^{-1} in LSR velocity for the [C II] 158 μm line channel, and from -670 to $+710$ kms^{-1} for the [O I] 63 μm line channel. The sampling intervals were chosen to be 20 and 24 kms^{-1}, respectively. The absolute sensitivity was calibrated by referring to Mars, which was assumed to be a 237 K blackbody (Lowenstein et al. 1977). Uncertainty of the absolute flux was estimated to be 30% due to the calibration errors and the inaccuracy of zero-level determination. The effective NEP of the system, including all losses of the optical system and the chopping efficiency, was 1×10^{-14} W Hz$^{-1/2}$ for [C II] 158 μm channel observations and 8×10^{-14} W Hz$^{-1/2}$ for [O I] 63 μm channel observations. For the calibration of the wavelength, we used the atmospheric lines of O_3 (157.61208 μm) and H_2O (158.28390 μm) in the [C II] channel and those of H_2O(63.456972 μm, 63.322487 μm) in the [O I] channel, which were incidentally present in the sweeping range. As a result, the velocity determination of better than 5 kms^{-1} was achieved. The common circular aperture corresponded to the beam diameters of 3′.4 (FWHM) or 3′.7 (equivalent disk) for [C II] 158 μm channel and 3′.5 (FWHM) or 3′.6 (equivalent disk) for [O I] 63 μm channel.

The secondary mirror was wobbled at 8 Hz, and the reference beam was offset in cross elevation direction by 15′.6 except the position $(l, b) = (-22'.0, -3'.8)$, where 8′ was used unintentionally. The reference beams were shifted to the south of the target positions. The observations were carried out at every 3′.6 along the ridge of the far-infrared continuum emission. Additional observations were also made on both sides of the ridge in the central region. The observed points are shown in Figure 1, together with the reference points, superposed on the far-infrared continuum emission map (Odenwald & Fazio 1984).

3. RESULTS

The spectral profiles of [C II] 158 μm line emission at all observed points are shown in Figure 2*a* for the central region, in Figure 3 for the extended wings from the central region and Figure 4 for several peripheral points. Due to a little poorer detectivity, [O I] 63 μm line was detected or marginally detected only at several positions, and their line profiles are shown in Figure 5.

3.1. *Overall Behaviors of the* [C II] *Emission*

As seen in Figures 2a, 3, and 4, [C II] emission is strong and widely distributed in the Galactic central region. Longitudinal variation of the line intensities is plotted in Figure 6, where the 158 μm continuum intensity estimated from the flat level of the [C II] line spectra outside the line is also illustrated, together with the 40–250 μm continuum flux reproduced from Odenwald & Fazio (1984) for comparison. Three conspicuous peaks coincided with Sgr A, Sgr B1, and Sgr C are seen. The longitudinal dependence of the [C II] line intensity is similar to that of the far-infrared but different in detail. It is interesting that the peak at positive longitude is more correlated with Sgr B1 but not with Sgr B2, which is much stronger in the far-infrared continuum as well as in radio emission. The peak at Sgr C is also conspicuous, even stronger than Sgr B1 and forms a counter object to the Sgr B1 peak. The overall distribution is rather symmetrical with respect to the Galactic center, while many components in the Galactic center region, far-infrared continuum emission (e.g., Odenwald & Fazio 1984), molecular gases (e.g., Güsten 1989), and radio continuum (e.g., Handa et al. 1987) are distributed more or less biased to the positive longitudes.

The observed spectral profiles show appreciably broader velocity dispersion than the instrumental resolution of the spectrometer at most of the observed points. Particularly in the central region near Sgr A, the velocity dispersion is extremely wide, and some of the profiles are apparently split into multiple components. A longitude-velocity diagram of the [C II] emission line along the Galactic plane ridge is illustrated in Figure 7. The velocity structure basically follows the Galactic rotation, but, if looked in at detail, many spectral profiles show complicated structures with different velocity components. Some of the spectral profiles with sufficient S/N have been deconvolved by applying the MEM (Maximum Entropy Method) as proposed by Wilczek & Drapatz (1985). As shown in Figure 8, the intrinsic spectra around the Galactic center at $(-2'.9, -2'.3)$ and $(0'.4, 1'.0)$ thus obtained are clearly split into two distinct velocity components. The same procedure was applied to the Sgr C region, where the spectral profiles are also deconvolved into multiple components (Fig. 9). Even in the other spectra, the spectral profiles can be resolved into different velocity components by visual inspection, although the data qualities are not good enough to apply the MEM technique.

Using all these information, morphological data as well as the velocity data, the emission features can be identified to many known objects such as Sgr A, Sgr B1/B2, Sgr C, the arched filaments, the 50/20 kms^{-1} molecular clouds near Sgr A and some other features discovered by radio observations. Here we make a brief summary of the observed characteristics of each identified sources in relation to the other observations.

3.2. *Sagittarius A Region*

The strongest intensities of [C II] emission and [O I] emission are observed at the position of $(l, b) = (-2'.9, -2'.3)$ which corresponds to Sgr A West. The beam encompasses the cir-

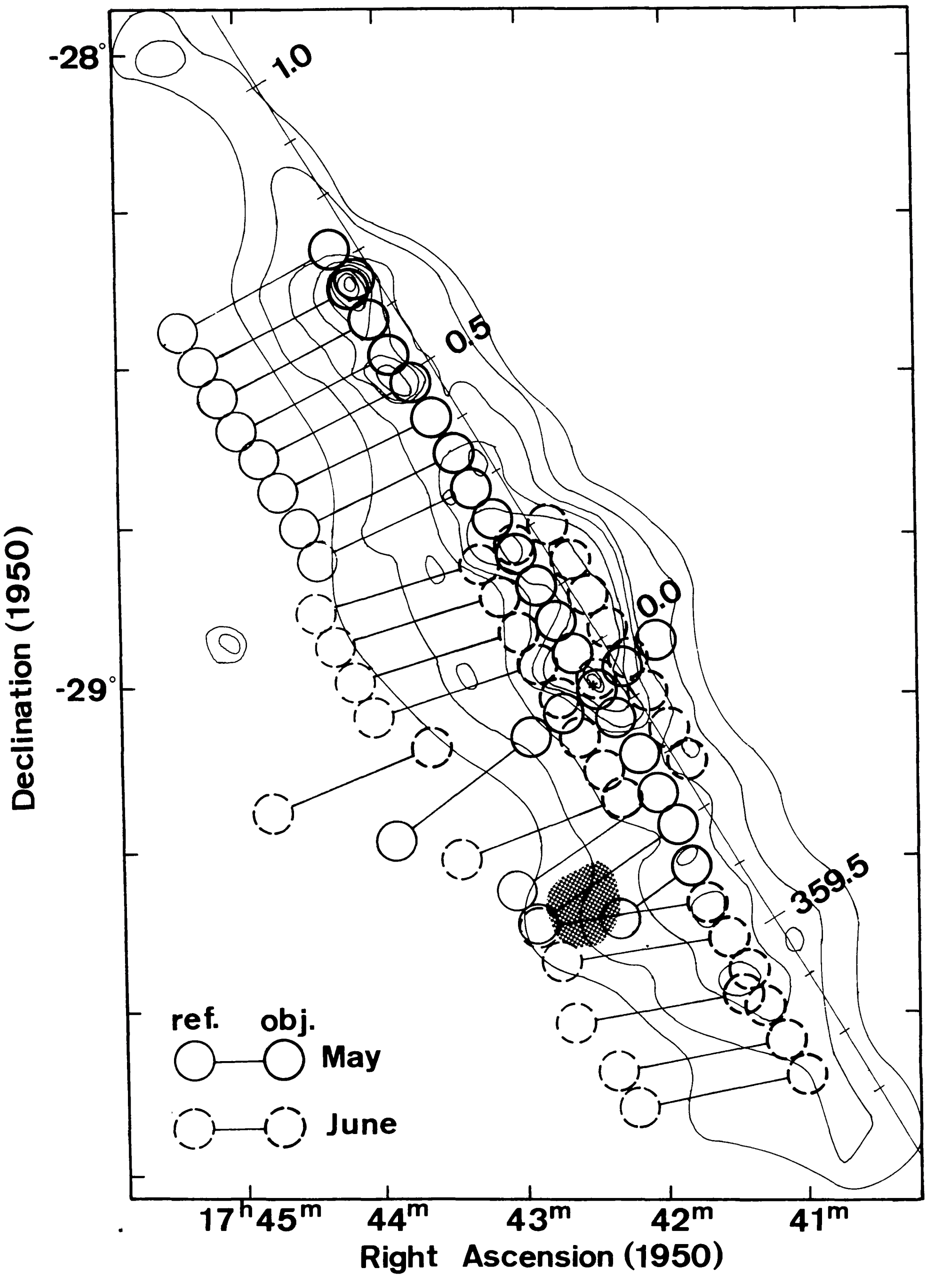

FIG. 1.—Observed positions (*bold circles,* May 25; *bold dashed* circles, June 5) and corresponding reference positions (*thin circles,* May 25; *thin-dashed circles,* June 5) on the 40–250 μm map by Odenwald & Fazio (1984). The contours are 1, 2, 4, 6, 8, 10, 20 and 40 times of 400 Jy per 1′ × 1.′5 beam. The shaded area represents the radio continuum source G-0.31−0.25.

cumnuclear disk (CND) surrounding the inner ionized region with a diameter of ∼3 pc. The nature of the CND, a rotating neutral gas and dust disk, has been revealed by a variety of observations as [C II] 158 μm, [O I]63 μm, [Si II]35 μm, far-infrared continuum, H I and several molecular lines (Güsten et al. 1987 and references therein). The deconvolved spectrum structure with two distinct velocity components of -70 kms^{-1} and +65 kms^{-1} (Fig. 8) is consistent with those obtained in these high spatial resolution observations, although the positive velocity component is relatively more intense than the negative one in our [C II] line spectrum.

The observed [C II] emission is much brighter than those obtained by GWCT and LGCT; our value of 1.7×10^{-10} W cm^{-2} sr^{-1} in the 3.′7 beam is comparable to the peak value of 1.7×10^{-10} W cm^{-2} sr^{-1} in the map made with 55″ beam by LGCT. This is obviously due to "self-chopping" effect unavoided in the LGCT observations with narrower chopping throws of 4′–6′ than 15.′6 of our observations. This indicates that [C II] emission is distributed extendedly. In this context, our results are also taken as lower limit. In fact, a finite intensity of [C II] emission of 2×10^{-11} W cm^{-2} sr^{-1} is observed even at the point of (l, b) = (−0.′4, −18.′4).

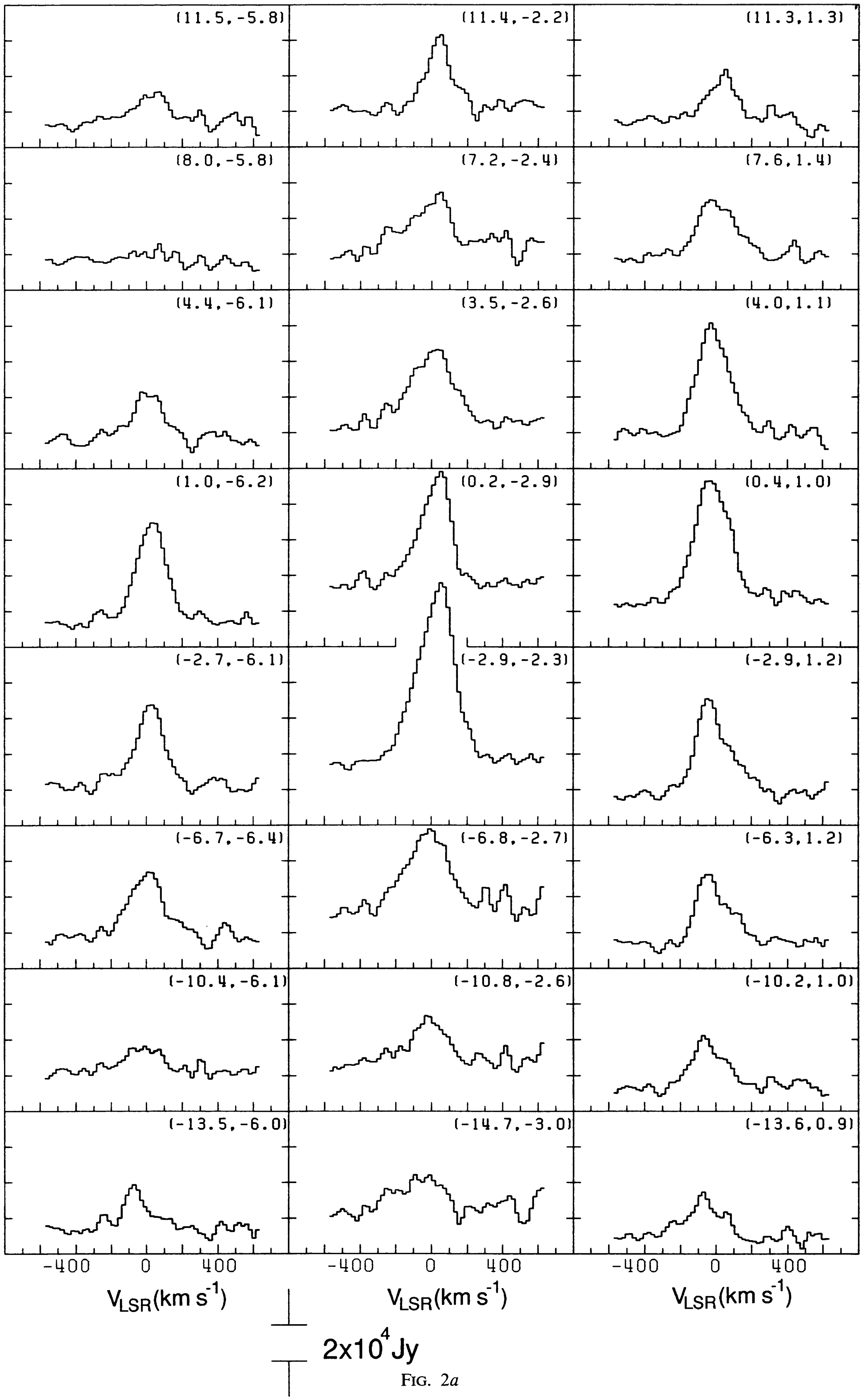

FIG. 2*a*

FIG. 2.—(*a*), [C II] 158 μm line spectra around the Galactic center. Positions are represented in arcminute of the Galactic cordinate (*l, b*). (*b*) The schematic 10 GHz radio continuum map (*thin full lines*) and NH_3 map (*dashed lines*) in the center are rewritten from Pauls et al. (1976) and Güsten, Walmsley, & Pauls (1981), respectively. The beams of our observations are represented by circles. North is up and east is to the left in the map. The position of the Galactic center is shown by an asterisk.

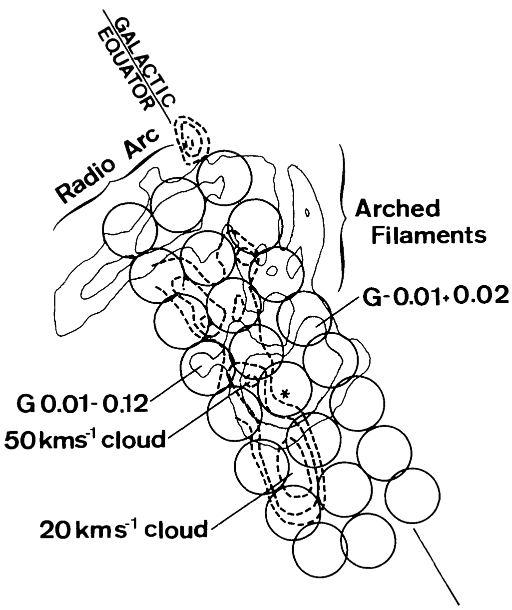

FIG. 2*b*

FIG. 2—*Continued*

On the other hand, the [O I] flux of 3×10^{-16} W cm^{-2} is consistent with the integrated flux of $\sim 4.5 \times 10^{-16}$ W cm^{-2} inside the lowest contour ($\sim 3'$ diameter) of GWCT. The [O I] line emission should not be so much extended as the [C II] emission.

3.3. *Sagittarius B1 and B2*

[C II] emission shows a strong enhancement at the position of Sgr B1 (G0.5−0.0) and G0.6+0.0, but it is fairly weak at Sgr B2 (Fig. 10). The gradual increase of peak velocities of [C II] emission, from ~ 45 kms^{-1} at Sgr B1 to ~ 70 kms^{-1} at Sgr B2, agrees with those of radio recombination lines (Wilson et al. 1970; Reifenstein et al. 1970; Downes et al. 1980; Anantharamaiah & Yusef-Zadeh 1989). The total luminosity of the [C II] emission in Sgr B1 region amounts to 3×10^3 $L_\odot$, corresponding to 0.06% of the total far-infrared luminosity of 5×10^6 $L_\odot$ calculated from the map of Gatley et al. (1978). This [C II]/FIR ratio is higher than the other positive longitude part around Sgr B1 (see Fig. 6), but within the range of 0.2%–0.01% typically observed in Galactic H II regions (Crawford et al. 1985; Stacey et al. 1991).

A comparable brightness of [C II] emission as Sgr B1 was observed at G0.6+0.0, where [O I] emission was marginally detected with an intensity of $\sim 6 \times 10^{-17}$ W cm^{-2}. The [O I]/[C II] ratio is ~ 1. The total luminosity of [O I] and [C II] lines within 3.'7 beam is ~ 0.1% of the far-infrared luminosity of 3×10^6 $L_\odot$.

The [C II] intensity at Sgr B2 is unexpectedly small compared to Sgr B1, although the former is one of the brightest sources in far-infrared as well as radio emission. The [C II]/FIR ratio is ~ 0.01%, substantially smaller than the typical values of Galactic H II regions.

3.4. *Sagittarius C*

Another prominent peak has been found at the position of Sgr C. Next to Sgr A, it has a stronger intensity than Sgr B1 peak. The peak position, $(l, b) = (-36.'3, -4.'9)$, is located a little south of the radio continuum peak $(-33.'7, -4.'9)$ (see Fig. 9). The spectral profiles deconvolved by the MEM processing are clearly split into two velocity components: low-velocity (roughly −60 km s^{-1}) and high-velocity (roughly −170 km s^{-1}) components. The low-velocity component is mainly associated with Sgr C, while the high-velocity component becomes dominant with decreasing longitude. It is important to note that the latter component is persistently present also toward positive longitude up to $l = -14.'7$ with gradual decrease of velocities.

In far-infrared continuum, Sgr C shows no noticeable concentration (Gatley et al. 1978; Odenwald & Fazio 1984), and hence its boundary is not definitely determined. Therefore, only a rough comparison of the intensities of [C II] emission and far-infrared emission is possible. Using the flux of the low-velocity component at the position $(l, b) = (-34.'4, -6.'0)$ as a representative to Sgr C, the [C II]/FIR ratio is estimated to be ~ 0.08%, almost compatible to that of Sgr B1.

3.5. *Arched Filaments*

Another enhancement of the [C II] intensity is seen near Sgr A at positive latitude ($b = 1'$) (see Fig. 2*a*). This corresponds to the radio features G − 0.01+0.02 and the arched filaments between Sgr A and the Radio Arc discovered by Pauls et al. (1976) and later resolved into very fine filamentary structures through VLA observations (e.g., Morris & Yusef-Zadeh 1989). The spectral profiles have two velocity components, −50 kms^{-1} and 50 kms^{-1} at $(l, b) = (0.'4, 1.'0)$, as shown in the MEM deconvolved spectra in Figure 8. The negative velocity component is dominant and spreads to positive and negative longitudes, and the velocity changes from −70 kms^{-1} at $l = -13.'6$ to −30 kms^{-1} at $l = 7.'6$. The kinematic structure of the negative velocity component agrees with the velocities observed by radio recombination lines of the H II regions (Pauls et al. 1976; Pauls & Mezger 1980; Anantharamaiah & Yusef-Zadeh 1989). The positive velocity component is relatively weak and shows a peak velocity of 50 kms^{-1} at $l = 11.'3$ and continues to the component at velocity of ~ 60 kms^{-1} at $l = -13.'6$. These characteristics of the positive and negative velocity components are clearly seen in the CS (1–0) observations by Tsuboi et al. (1989).

3.6. 50 km s^{-1} *and* 20 km s^{-1} *Clouds*

At the negative latitude side of the Galactic center region, there is also some enhancement in the [C II] intensity. The region is apparently overlapped with the 50 and 20 kms^{-1} molecular clouds (see Fig. 2b). The velocity profiles of the [C II] emission contain the same velocity components and are consistent with those observed in the molecular clouds (Güsten & Downes 1980; Güsten, Walmsley, & Pauls 1981; Güsten & Henkel 1983; Armstrong & Barrett 1985; Sandqvist 1989; Okumura et al. 1989). This component is dominant at the positions of $(l, b) = (1.'0, -6.'2)$, $(-2.'7, -6.'1)$ and $(-6.'7,$

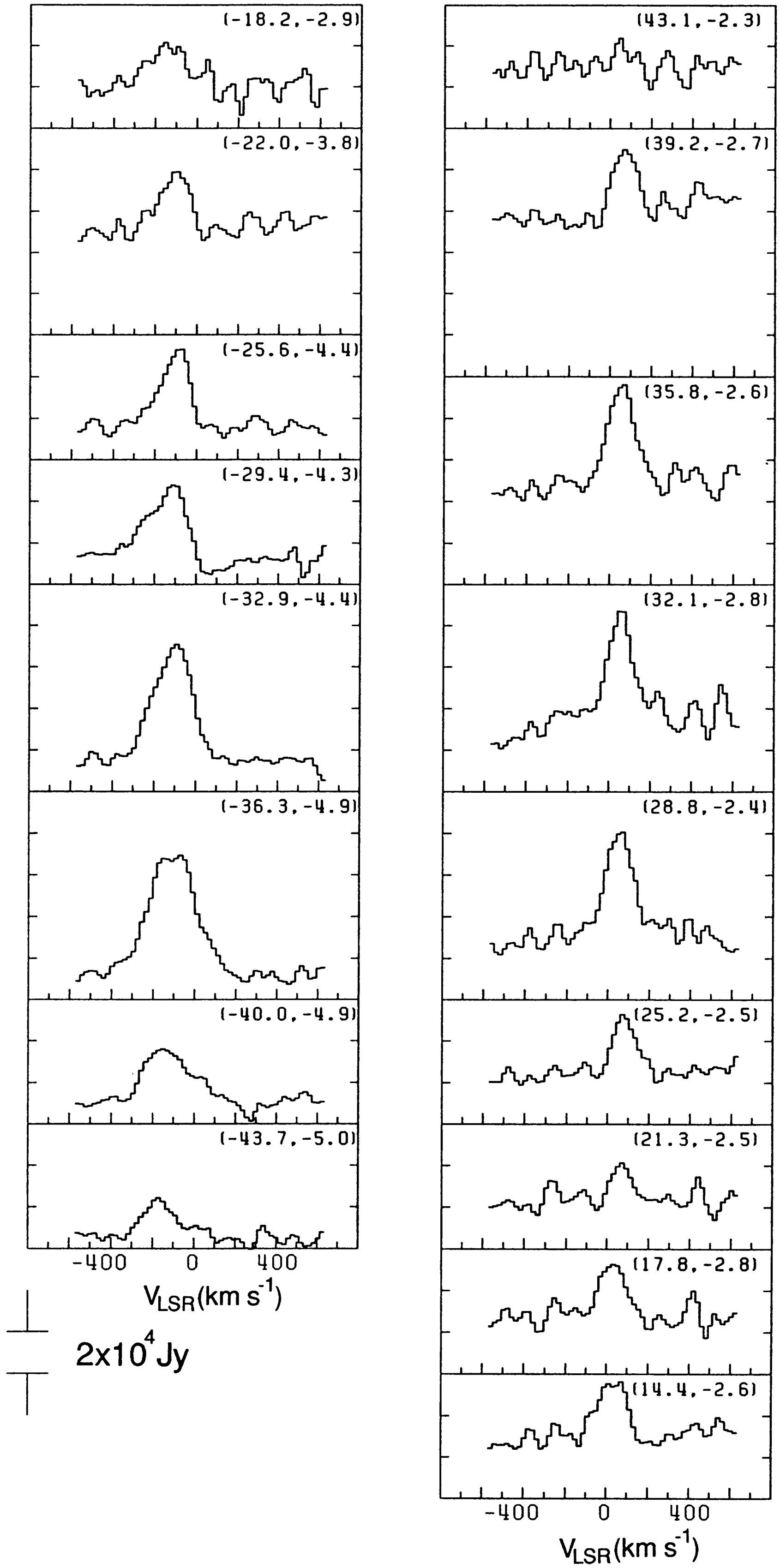

FIG. 3.—Same as Fig. 2*a*

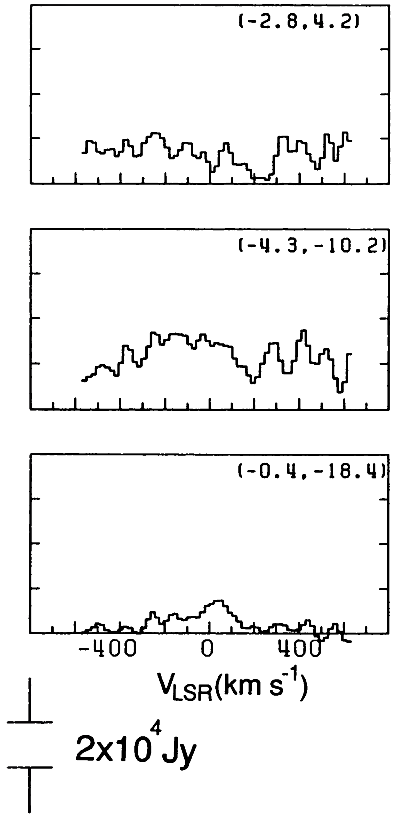

FIG. 4.—Same as Fig. 2*a*

−6'.4), south and east of the Galactic center region. The existence of the 50 kms^{-1} component is evidently shown in the finer resolution observations of the Galactic center region by Genzel et al. (1990). The [C II] emission from the northern part of the 20 kms^{-1} cloud is also seen in the map by Poglitsch et al. (1991).

3.7. *General Diffuse Emission*

In addition to the [C II] emission attributed to individual sources, there apparently exist some more components. In fact, substantial emission is present at the gaps between the Galactic center and Sgr B1 peak as well as between the Center and Sgr C peak, where no noticeable H II regions or molecular clouds are found. A finite intensity of [C II] emission is also observed even at (l, b) = (−0'.4, −18'.4) only where we made an observation of a place far from the Galactic ridge. These results show that the diffuse [C II] emission spreads in a wide area over the Galactic center region.

4. DISCUSSION

Strong [C II] emission has been observed in the Galactic central region by a balloon-borne telescope. The longitudinal dependence of the intensity resembles with those of far-infrared emission and radio continuum emission, but with some deviation in details. Morphologically, the emission is more or less associated either with H II regions or molecular clouds.

Three intensity peaks correspond with Sgr A, Sgr B1, and

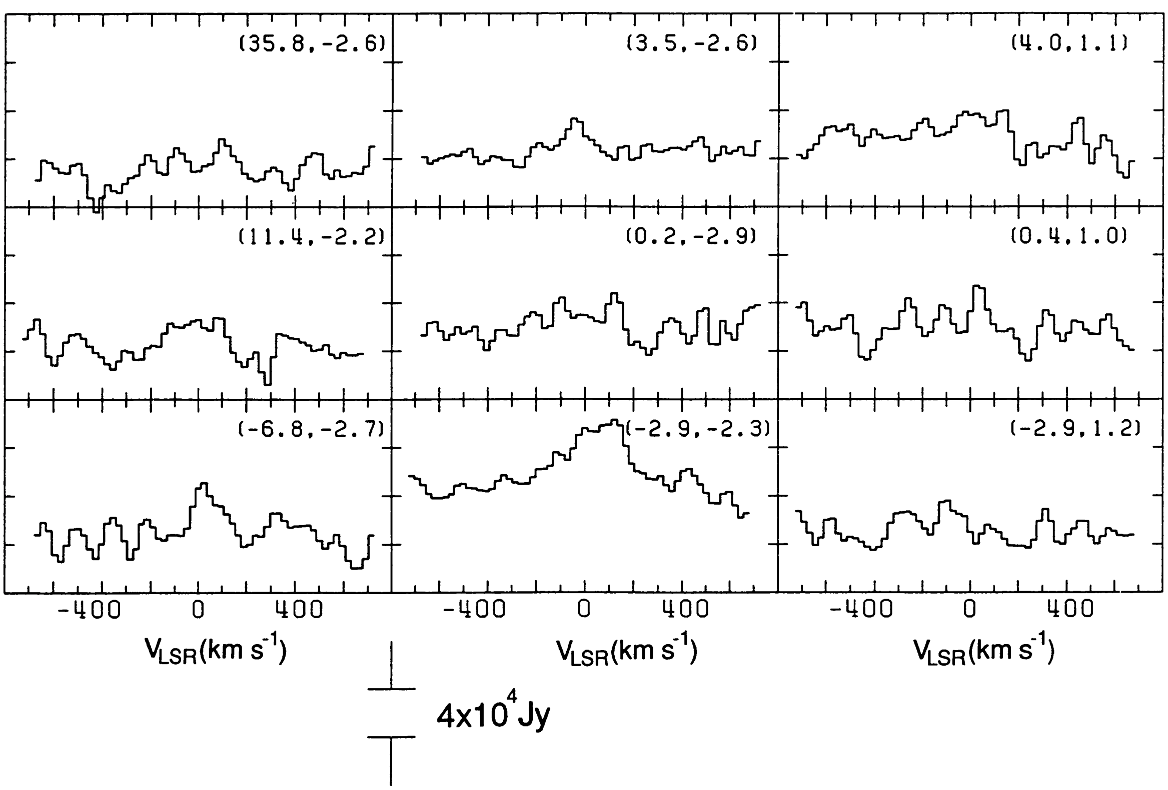

FIG. 5.—The detected or marginally detected [O I]63 μm line spectra around the Galactic center

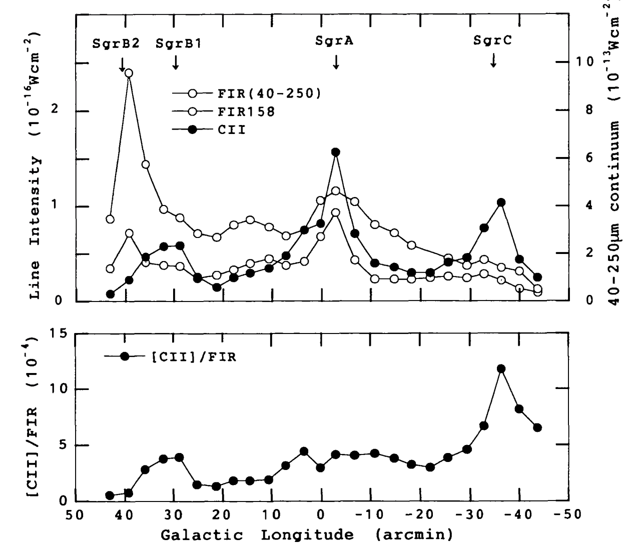

FIG. 6.—*Top:* the distributions of the velocity-integrated [C II] 158 μm line, the 158 μm continuum, and the 40–250 μm continuum (Odenwald & Fazio 1984) on the ridge along the Galactic longitude. *Bottom:* [C II] 158 μm to (40–250 μm) continuum ratios distribution.

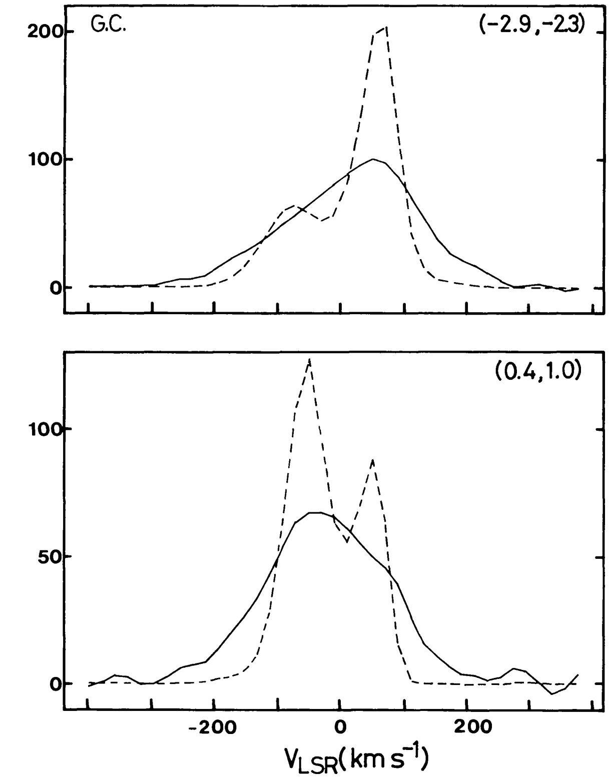

FIG. 8.—The observed [C II] 158 μm lines (*solid line*) and MEM deconvolved spectra (*dashed line*) at Sgr A West and (0′.4, 1′.0). The deconvolution is applied to the line component after subtracting the continuum.

Sgr C. The two side peaks are distributed symmetrically with the Galactic center.

The observed velocity field pattern (Fig. 7) is similar to that observed in the atomic recombination lines and molecular lines (e.g., Kesteven & Pedlar 1977; Gusten 1989). From the morphological correspondence and the velocity field pattern, we can identify some of the observed emission regions to previously known objects. In addition to these individual sources, there is a general diffuse component seen between the emission peaks, where no identifiable sources are present.

In the following, a few comments are added to each individual sources.

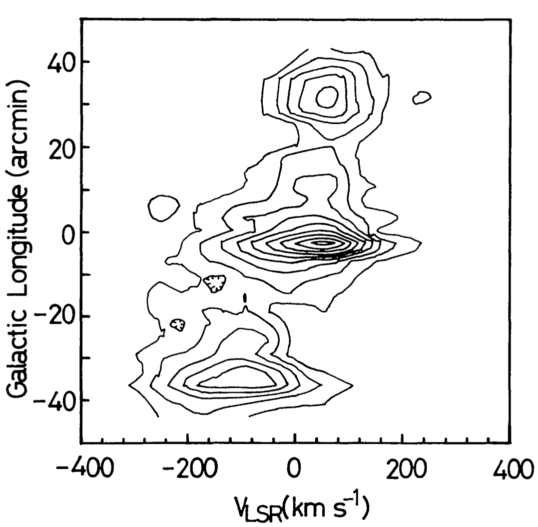

FIG. 7.—The velocity-position map of the [C II] 158 μm line along the ridge of the Galactic center. The contour levels are 0.1, 0.2, . . . , 0.9 of the peak value at Sgr A West.

4.1. *Sagittarius A region*

The [C II] emission is the strongest at Sgr A West, but some additional components are extended to the north. The latter is apparently associated with the arched filaments (e.g., Morris & Yusef-Zadeh 1989). The correspondence is also seen in the velocity profile. In the south of Sgr A West, another source is identified as the 50 and 20 kms^{-1} molecular clouds from its common position and velocity profile.

Detailed observations have been reported by Genzel et al. (1990), Poglitsch et al. (1991), and Erickson et al. (1991). Their observations were made with a smaller beam and a higher spectral resolution, and therefore some fine structures have been resolved. In general, the present observations agree with their results.

4.2. *Sagittarius B1/B2 Region*

A conspicuous emission peak is located at the position of Sgr B1, not at Sgr B2. This is an interesting results because Sgr B2 excels Sgr B1 in almost every respect of various emissions and activities. Two possibilities are considered. One is that [C II] emission which has been emitted in the core of Sgr B2 is absorbed by the thick dust clouds. In fact, an extremely large optical depth of $\tau \sim 1$ is observed in the far-infrared region (e.g., Thronson & Harper 1986) toward the hot core of Sgr B2. However, Sgr B2 extends widely, and therefore the average optical depth should be much less than that of the core. This means that either the generation of [C II] emission in Sgr B2 is

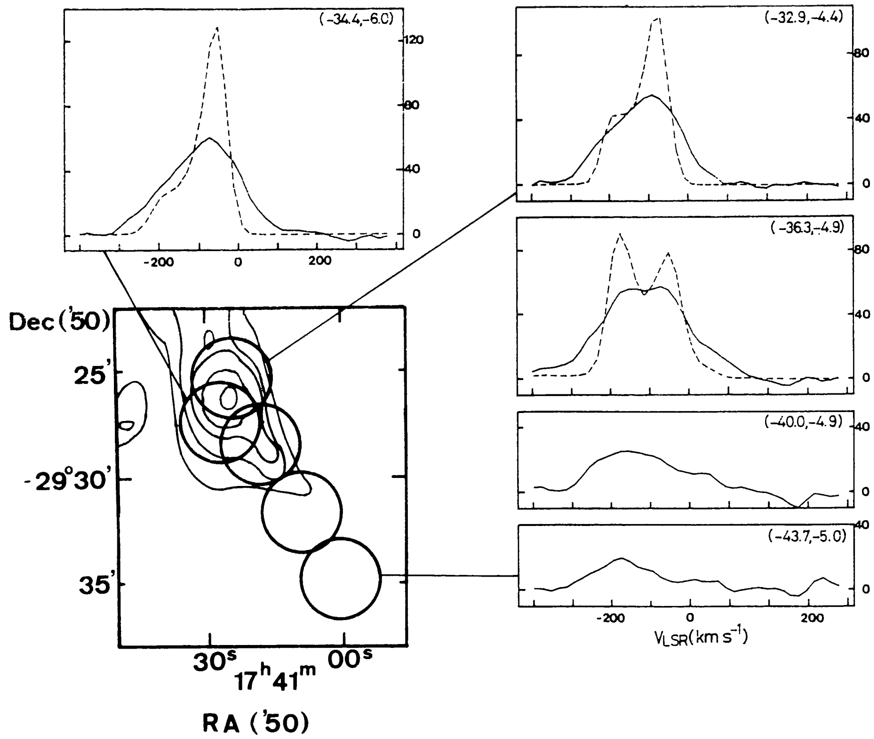

FIG. 9.—[C II] 158 μm line spectra in Sgr C region after subtracting the continuum. The contour is a 10 GHz radio continuum map rewritten from Downes et al. (1979). The observed [C II] 158 μm lines and MEM deconvolved spectra are shown by a solid line and a dashed line, respectively.

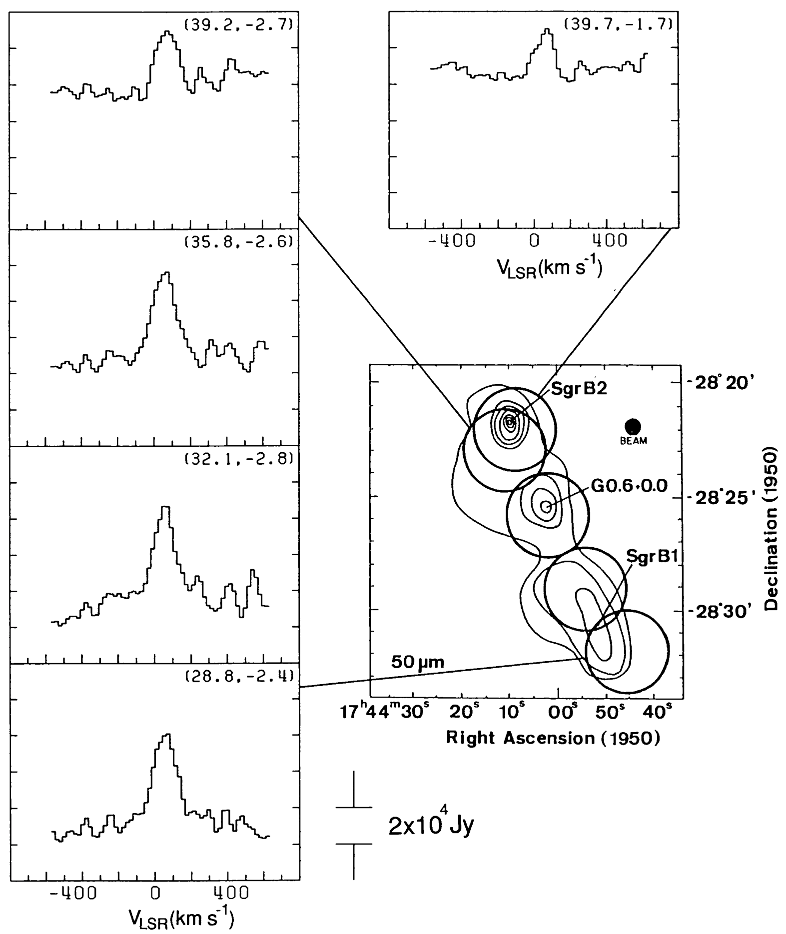

FIG. 10.—[C II] 158 μm lines spectra in Sgr B1 and B2 region. The contour is a 50 μm continuum map (Gatley et al. 1978).

concentrated in the core region and thus invisible due to the absorption or the emission is intrinsically weak as a whole. Another possibility is that Sgr B1 is a neighbor (located at the edge of) to Sgr B2 and the surface of Sgr B2 cloud is illuminated in the Sgr B1 side. This idea is not inconsistent in terms of the common velocity pattern in Sgr B1 and Sgr B2.

4.3. *Sagittarius C Region*

This region's strongest peak is next to SgrA; however, SgrC is associated with neither H II region nor radio emission as prominent as Sgr A or Sgr B2. The velocity profile is clearly resolved into two components: low (-60 km s^{-1}) and high (-170 km s^{-1}) velocities. The former velocity component coincides with Sgr C (peaking at the maximum intensity point of the radio continuum), while the latter component has its maximum at the negative longitude side of Sgr C. It is interesting to note that the velocity of the latter component is compatible to that of the expanding molecular ring (Scoville 1972; Kaifu, Kato, & Iguchi 1972). This might indicate that the high-velocity component is associated with the expanding molecular ring. This velocity components is traced till $l = -14\farcm7$ on the Galactic plane ridge.

The [C II]/FIR ratios around Sgr C show high values. The ratio at ($-36\farcm3$, $-4\farcm9$) is estimated to be 0.14% by a comparison of velocity-integrated [C II] emission and far-infrared luminosity derived from Galactic plane images of *IRAS,* which is compatible to an upper bound of the typical values of the Galactic sources.

The peak positions of the two components almost coincide with large molecular clouds seen in the map of integrated CO intensity map made by Stark et al. (1989). The location of the maximum intensity of [C II] emission is, however, shifted slightly toward the Galactic center, as if they are emitted at the surface of the molecular clouds facing to the Galactic center. If this is really the case, it may means that a substantial part of UV radiation is supplied by the Sgr A complex.

4.4. *Diffuse Component*

Besides the bright individual sources, there remains some component which is not attributed to discrete sources. In the intensity minimum, but finite, between the three peaks, no noticeable sources of far-infrared or radio continuum are found. The emission may come from many unresolved compact sources or diffusely distributed ELD region.

Physical characteristics of each component are summarized in Table 1.

4.5. *Overall Characteristics of the Emission*

Although the [C II] emission is strongly observed in the Galactic central region, the relative intensities are weak compared to the typical Galactic sources. In fact, the average [C II]/FIR ratio is 0.06%, which almost corresponds to the minimum values ever observed in the Galactic and extragalactic sources (Stacey et al. 1991). Only in the Sgr C region are higher ratios observed.

As for the observable points of [O I] emission, the [O I]/[C II] ratio is less than 3, a typical value of the normal Galactic sources. This indicates that the emission is favorably supplied from photodissociation regions and shock-induced emission should be negligible. A larger ratio of ~ 10 has been observed in the circumnuclear disk (CND) of the Sgr A by Genzel et al. (1985), but it should have been smeared out in our observations by the ambient regions with lower ratios.

The total flux of [C II] emission in the observed area [25 beams on the Galactic plane ridge and $2 \times$ (8 beams) of the side band in the central region] is 2.1×10^{-15} W cm^{-2}. With assumptions of a density of 5×10^3 cm^{-3}, a temperature of 200 K, and the C^+ ion abundance ratio of 3×10^{-4}, the total gas mass associated with C^+ region turns to be $4 \times 10^4 M_\odot$. On the other hand, referring to the optical depth of the far-infrared continuum, the total gas mass is estimated to be as large as $1 \times 10^6 M_\odot$ according to Hildebrand (1983) and on an assumption of a gas-to-dust mass ratio of 100. Hence, $\sim$4% of the gas mass in the Galactic central region is shared by the photodissociation region. The derived fraction is compatible with the 5% estimated in the Sgr A region by Poglitsch et al. (1991), but substantially smaller than the values of 30%–50% estimated for the diffuse component in the Galactic plane by Shibai et al. (1991).

As for the UV sources to ionize and energize the emission region, the contribution of young and high-temperature stars

TABLE 1

Observed Data and Derived Parameters in Typical Sources

Position	(l, b)	[C II] 158 μm (10^{-17} W cm^{-2})	[O I] 63 μm / [C II] 158 μm	[C II] 158 μm / FIR	n[a] (cm^{-3})	T[a] (K)	N[C^+] (cm^{-2})	Gas mass ($M_\odot$) in the C^+ Region	References[b]
Galactic center	($-2\farcm9$, $-2\farcm3$)	15.7	1.8	5×10^{-4}	1×10^4	250	1.5×10^{18}	2700	1
G0.01–0.12	(1.0, −6.2)	7.7	<1	7×10^{-4}	5×10^3	200	8×10^{17}	1500	1
Arched filaments	(4.0, 1.1)	8.4	~1	4×10^{-4}	1×10^4	200	8×10^{17}	1500	1
Sgr B1	(28.8, −2.4)	5.9	<1.5	7×10^{-4}	5×10^3	200	6×10^{17}	1100	2
Sgr B2	(39.7, −1.7)	1.5	<6	9×10^{-5}	5×10^3	200	1.6×10^{17}	300	3
Sgr C[c]	(−34.4, −6.0)	8.4	<1	11×10^{-4}	5×10^3	200	9×10^{17}	1600	4
		~6.5	<1.5	8×10^{-4}	5×10^3	200	7×10^{17}	1300	4
	(21.3, −2.5)	1.5	<6	2×10^{-4}	5×10^3	200	1.6×10^{17}	300	4
	(−14.7, −3.0)	3.6	<3	5×10^{-4}	5×10^3	200	4×10^{17}	700	4
Total observed area		210	<2	6×10^{-4}	5×10^3	200	6×10^{17}	40000	4

[a] Assumed hydrogen density and kinematic temperature to deduce column density of C^+ and gas mass of C^+ region in our $3\farcm7$ beam.
[b] References for FIR: (1) Dent et al. 1982; (2) Gatley et al. 1978; (3) Thronson & Harper 1986; (4) *IRAS* Survey.
[c] The expected Sgr C component after subtracting the high-velocity component.

should be substantial. If the UV sources were supplied mostly by early O stars, they should be luminous enough to be observed as discrete sources in previous far-infrared surveys. But this was not the case. In fact, Odenwald & Fazio (1984) have claimed that most of the energy source to the far-infrared continuum is supplied by stars later than O8. This indicates that the UV radiation is supplied not by a small number of high-luminosity sources but by many moderately luminous sources such as late O and B stars. Poglitsch et al. (1991) have proposed that there is in the SgrA region a substantial contribution of strong UV radiation from the central core, based on the fact that much enhanced [C II] emission is found at the surface of molecular clouds facing toward the nuclear core. Mezger & Pauls (1979) have proposed the presence of ELD component in the Galactic center region extending to 110×70 pc. Diffuse UV radiation in this field would also contribute to the [C II] emission.

5. CONCLUSION

We have presented balloon-borne observations of the far-infrared fine structure lines of [C II] 158 μm and [O I] 63 μm in the Galactic center region of $|l| \leqq 0\overset{\circ}{.}7$. Intense [C II] emission has been detected at almost all of the observed positions and [O I] emission at several positions. Spectral profiles are resolved and kinematical characteristics of the [C II] emission gas in the Galactic central region have been also revealed. The intensity distribution shows three distinct peaks at Sgr A, Sgr B1, and Sgr C. These features, as well as some other less conspicuous ones, can be identified morphologically and kinematically to the H II regions or molecular clouds ever known from radio and far-infrared observations. Detailed comparison, however, show some discrepancies and deviation from simple relationships between the emissions, e.g., the reverse contrast between [C II] emission and far-infrared/radio continuum emissions in Sgr B1 and Sgr B2.

The total luminosity of the [C II] emission in the observed area is $5 \times 10^4\ L_\odot$, and the average [C II]/FIR ratio is 0.06%, which corresponds to almost the lowest limit ever observed in the Galactic and extragalactic sources (Stacey et al. 1991). This may be due to the excessive UV radiation, as seen in the midst of the active H II regions.

So far as the observable points are concerned, [O I]/[C II] ratios are less than 3 (see Table 1); thus, the emission can be generated in photodissociation regions, the UV sources of which are supplied by more extendedly distributed O and B stars, but the contribution of the luminous UV object of the Galactic nucleus may noticeable in the Sgr A region.

The fractional mass contribution of the [C II] region is $\sim$4% of the total gas mass, relatively smaller than the diffuse component observed in the general Galactic plane (Shibai et al. 1991).

The high-velocity component (-170 km s^{-1}) observed near and around Sgr C should correspond to that observed in the expanding molecular ring. It may suggest their physical connection.

We are grateful to the staff of NSBF in Palestine for their expertise support. We thank H. Takami, M. Narita, and the Balloon group of ISAS for developing the instrument with us. We also thank M. Tsuboi and T. Nagata for useful discussions and communicating results prior to the publications. This research has been supported by grants-in-aid from the Ministry of Education, Science, and Culture in Japan, by the Japan Society for the Promotion of Science, and by the National Science Foundation in the US (Grant No. INT-8613481).

REFERENCES

Anantharamaiah, K. R., & Yusef-Zadeh, F. 1989, in IAU Symp. 136, The Center of the Galaxy, ed. M. Morris (Dordrecht: Reidel), 159
Armstrong, J. T., & Barrett, A. H. 1985, ApJS, 57, 535
Brown, R. L., & Liszt, H. S. 1984, ARA&A, 22, 223
Cox, P., & Laureijs, R. 1989, in IAU Symp. 136, The Center of the Galaxy, ed. M. Morris (Dordrecht: Reidel), 121
Cox, P., & Mezger, P. G. 1988, in Lecture Note in Physics, vol. 297, Comet to Cosmology, ed. A. Lawrence (Berlin: Springer), 97
Crawford, M. K., Genzel, R., Townes, C. H., & Watson, D. M. 1985, ApJ, 291, 755
de Jong, T., Dalgarno, A., & Boland, W. 1980, A&A, 91, 68
Dent, W. A., Werner, M. W., Gatley, I., Becklin, E. E., Hildebrand, R. H., Kene, R. H., & Whitcomb, S. E. 1982, in AIP Conf., 83, The Galactic Center, eds. G. R. Riegler & R. D. Blandford (New York: AIP), 33
Downes, D., Goss, W. M., Schwartz, U. J., & Wouterloot, J. G. A. 1979, A&AS, 35, 1
Downes, D., Wilson, T. L., Bieging, J., & Wink, J. 1980, A&AS, 40, 379
Erickson, E. F., Colgan, S. W. J., Simpson, J. P., Rubin, R. H., Morris, M., & Haas, M. R. 1991, ApJ, 370, L69
Gatley, I., Becklin, E. E., Werner, M. W., & Harper, D. A. 1978, ApJ, 220, 822
Genzel, R., Harris, A. I., & Stutzki, J. 1989, in ESLAB Symp., 22, Infrared Spectroscopy in Astronomy, ed. B. H. Kadeich, ESA SP-290 (Noordjwik) 115
Genzel, R., Stacey, G. J., Harris, A. I., Townes, C. H., Geis, N., Graf, U. U., Poglitsch, A., & Stutzki, J. 1990, ApJ, 356, 160
Genzel, R., Watson, D. M., Crawford, M. K., & Townes, C. H. 1985, ApJ, 297, 766 (GWCT)
Genzel, R., Watson, D. M., Townes, C. H., Dinerstein, H. L., Hollenbach, D., Lester, D. F., Werner, M., & Storey, J. W. V. 1984, ApJ, 276, 551
Güsten, R. 1989, in IAU Symp. 136, The Center of the Galaxy, ed. M. Morris (Dordrecht: Reidel), 89
Güsten, R., & Downes, D. 1980, A&A, 87, 6
Güsten, R., Genzel, R., Wright, M. C. H., Jaffe, D. T., Stutzki, J., & Harris, A. I. 1987, ApJ, 318, 124
Güsten, R., & Henkel, C. 1983, A&A, 125, 136
Güsten, R., Walmsley, C. M., & Pauls, T. 1981, A&A, 103, 197
Handa, T., Sofue, Y., Nakai, N., Hirabayashi, H., & Inoue, M. 1987, PASJ, 39, 709
Heiligman, G. M. 1987, ApJ, 314, 747
Hildebrand, R. H. 1983, QJRAS, 24, 267
Kaifu, N., Kato, T., & Iguchi, T. 1972, Nature Phys. Sci., 238, 105
Kesteven, M. J., & Pedlar, A. 1977, MNRAS, 180, 731
Lowenstein, R. F., et al. 1977, Icarus, 31, 315
Lugten, J. B., Genzel, R., Crawford, M. K., & Townes, C. H. 1986, ApJ, 306, 691 (LGCT)
Mezger, P. G., & Pauls, T. 1979, in IAU Symp. 84, The Large-Scale Characteristics of the Galaxy, ed. W. B. Burton (Dordrecht: Reidel), 357
Morris, M., & Yusef-Zadeh, F. 1989, ApJ, 343, 703
Nakagawa, T., Okuda, H., Shibai, H., Kobayashi, Y., & Matsuhara, H. 1990, in Proc. SPIE, Instrumentation in Astronomy VII, vol. 1235, 97
Odenwald, S. F., & Fazio, G. G. 1984, ApJ, 283, 601
Okuda, H., et al. 1984, in Proc. 14th Internat. Symp. on Space Technology and Science, vol. 14, ed. M. Nagatomo (Tokyo: AGNE), 1217
Okuda, H., et al. 1989, in IAU Symp. 136, The Center of the Galaxy, ed. M. Morris (Dordrecht: Reidel), 145

Okuda, H., Shibai, H., Nakagawa, T., Kobayashi, Y., Matsumoto, T., Low, F. J., & Nishimura, T. 1986, in Proc. of SPIE, 627, Instrumentation in Astronomy VI, vol. 627, 20

Okumura, S. K., et al. 1989, ApJ, 347, 240

Pauls, T., Downes, D., Mezger, P. G., & Churchwell, E. 1976, A&A, 46, 407

Pauls, T., & Mezger, P. G. 1980, A&A, 85, 26

Poglitsch, A., Stacey, G. J., Geis, N., Haggerty, M., Jackson, J., Rumitz, M., Genzel, R., & Townes, C. H. 1991, ApJ, 374, L33

Reifenstein III, E. C., Wilson, T. L., Burke, B. F., Mezger, P. G., & Altenhoff, W. J. 1970, A&A, 4, 357

Sandqvist, As. 1989, A&A, 223, 293

Scoville 1972, ApJ, 175, L127

Shibai, H., et al. 1990, in Proc. of SPIE, 1235, Instrumentation in Astronomy VII, 108

———. 1991, ApJ, 374, 522

Sofue, Y. 1989, in IAU Symp. 136, The Center of the Galaxy, ed. M. Morris (Dordrecht: Reidel), 213

Stacey, G. J., Geis, N., Genzel, R., Lugten, J. B., Poglitsch, A., Sternberg, A., & Townes, C. H. 1991, ApJ, 373, 423

Stacey, G. J., Viscuso, P. J., Fuller, E. F., & Kurtz, N. T. 1985, ApJ, 289, 803

Stark, A. A., Bally, J., Wilson, R. W., & Pound, M. W. 1989, in IAU Symp. 136, The Center of the Galaxy, ed. M. Morris (Dordrecht: Reidel), 129

Thronson, H. A., & Harper, D. A. 1986, ApJ, 300, 396

Tielens, A. G. G. M., & Hollenbach, D. 1985, ApJ, 291, 722

Tsuboi, M., Handa, T., Inoue, M., Inatani, J., & Ukita, N. 1989, in IAU Symp. 136, The Center of the Galaxy, ed. M. Morris (Dordrecht: Reidel), 213

Wilczek, R., & Drapatz, S. 1985, A&A, 142, 9

Wilson, T. L., Mezger, P. G., Gardner, F. F., & Milne, D. K. 1970, A&A, 6, 364